

# Explaining Mammographic Texture: The Role of View and Abnormality Type in Early Cancer Diagnosis

Bianca Iacob<sup>a</sup> and Laura Diosan<sup>b</sup>

Faculty of Mathematics and Computer Science, University Babeş Bolyai, Cluj-Napoca, Romania  
{andreea.lixandru, laura.diosan}@ubbcluj.ro

**Keywords:** Textural Feature, CNN, Mammogram, Early Diagnosis, Breast Cancer.

**Abstract:** Detecting breast cancer at an early stage significantly increases the chances of successful treatment and survival. Understanding the full topology of various abnormalities requires analyzing multiple mammography views. This study evaluates the performance of mammographic views in detecting abnormalities, focusing on calcifications and masses, to enhance early cancer diagnosis. By examining the importance of considering both the type of abnormality and the mammographic view, we aim to identify key factors influencing detection accuracy. Additionally, we investigate whether incorporating textural features such as GLCM, GLRLM, and GLSZM can improve overall model performance. Our findings underscore the necessity of a tailored approach in mammographic analysis. These insights are crucial for advancing early diagnostic capabilities and improving patient outcomes.

## 1 INTRODUCTION

The craniocaudal (CC) and mediolateral oblique (MLO) views are two standard perspectives used in mammography, each offering distinct advantages and limitations in breast cancer detection and characterization (Vachon et al., 2007). In the CC view, the breast is compressed from above to below. The X-ray beam is directed from the head (cranio) to the foot (caudal). It provides a clear image of the central and medial parts of the breast. The advantage of this view is that it allows a better visualization of the medial breast tissue. The limitation is that it may not capture some areas in the upper outer quadrant and the axillary tail region (Duffy et al., 2008). In the MLO view, the breast is compressed diagonally, from the upper outer part (superior-lateral) to the lower inner part (inferior-medial). The X-ray beam is directed at an angle, usually around 45 degrees (Kim SJ, 2006). It provides a more comprehensive view of the breast, including the upper outer quadrant and the axillary tail, which are common sites for breast cancer. This view offers better visualization of the upper outer quadrant and axillary tail. It can be more challenging to obtain a consistent angle and positioning, potentially leading to variability in image quality (Kala and Ezhilarasi, 2018).

In mammography, abnormalities include masses and calcifications. A mass is a distinct area of breast tissue that may have well-defined or ill-defined edges; spiculated margins (jagged or star-like edges) are more indicative of malignancy (Bassett, 1992). Calcifications are small calcium deposits visible as white spots on a mammogram. Macrocalcifications, larger and coarser, are typically benign and linked to aging or prior injuries, requiring no further workup. Microcalcifications, smaller and finer, may be benign or malignant.

There are two arguments as the basis of our investigation. On one hand, (Araque et al., 2019) showed that the early warning signs of cancer manifest differently in MLO and CC views. On the other hand, medical professionals favor the MLO view in clinical practice for its comprehensive coverage of breast tissue. Detecting the chest wall to exclude the pectoral muscle in MLO images adds preprocessing time, and inaccurate delineation can introduce noise and errors in feature extraction. In this context, this paper aims to investigate the impact of employing MLO or CC mammographic views and to offer experimental evidence in support of the choice of mammographic views for breast cancer identification.

Our study addresses a significant gap in the existing literature, which is the lack of detailed analyses on the choice of mammographic view (CC or MLO) for automatically discriminating between benign and

<sup>a</sup>  <https://orcid.org/0009-0006-9765-6410>

<sup>b</sup>  <https://orcid.org/0000-0002-6339-1622>

malignant breast lesions. While mammography is widely regarded as the gold standard for breast cancer screening<sup>1</sup> especially due to its ability to detect microcalcifications, there is insufficient justification in the literature for the preferred view in computerized analysis. The majority of authors have based their analysis on both views for breast cancer risk assessment (Abdoell et al., 2020; Sasikala and Arun Kumar, 2024) or for breast cancer classification (malign vs. benign) (Cui et al., 2021). Only a few authors have analyzed the importance of MLO and CC views, and only in the context of breast cancer risk assessment (Astrid Padilla, 2021) or for discriminating between images from healthy patients and those with cancer (Tan et al., 2016; Pérez-Benito et al., 2019). To the best of our knowledge, there is no study dedicated to evaluating breast cancer classification using just one view and texture features extracted from the mammograms. Our research aims to systematically evaluate the impact of using MLO and CC mammographic views on the accuracy of breast cancer classification. By providing experimental evidence, we hope to offer clear guidance on the optimal choice of mammographic view for computerized analysis. Therefore, this paper aims to address the following research questions:

**RQ1.** In what ways do craniocaudal and MLO views differ in their accuracy, sensitivity and specificity for detecting breast cancer?

**RQ2.** Can mammographic images of calcifications and masses be combined without compromising the performance of diagnostic models, or is it necessary to differentiate between these types for optimal accuracy?

The paper will continue with Section 2 which contains the Related work, then we will have Section 3 which will present the dataset used, the pre-processing steps applied, the features used, the model involved and the training procedure. Section 4 will present the results obtained for the experiments performed based on the view of the mammogram, CC or MLO, and we will end up with the conclusions in Section 5.

## 2 RELATED WORK

Early detection of breast cancer, whether benign or malignant, is essential for improving the survival rate and increasing the quality of life of patients (Coughlin and Ekwueme, 2009). Early identification of tumors

allows rapid and less invasive medical interventions, thus reducing the risk of metastases and subsequent complications. In the case of benign cancer, early detection can prevent its transformation into malignant forms by ensuring proper monitoring and treatment. Regular screening, through methods such as mammograms and periodic self-examinations, plays a crucial role in detecting abnormalities at early stages, allowing for prompt and effective interventions, leading to better outcomes and an increased likelihood of complete cure (Charan et al., 2018).

The classical radiomics workflow is based on several important steps: image acquisition/reconstruction, image segmentation, feature extraction and quantification, and statistical analysis and model building. Segmentation problem can be done automatically, semi-automatically or manually (Van Timmeren et al., 2020).

Textural features focus on detecting local spatial configurations and intensity variations, aiding in tissue discrimination and malignancy detection. Unlike higher-order statistics, textural features effectively retain this localized spatial detail (Bajcsi and Chira, 2023). Additionally, they are robust (Singh et al., 2022) to variations in image acquisition and processing, making them valuable for clinical diagnosis and prognosis. Their computational efficiency is advantageous for rapid mammogram analysis in extensive screening programs (Siviengphanom et al., 2022).

Deep learning and machine learning algorithms have achieved accuracy in cancer diagnosis comparable to that of an average breast radiologist (Rodriguez-Ruiz et al., 2019). Deep learning systems, particularly Convolutional Neural Networks (CNNs), have shown performance on par with radiologists and can enhance their accuracy when used for decision support. CNNs have been effective in classifying mammograms into benign and malignant categories (Rodriguez-Ruiz et al., 2019; Mahmood et al., 2022). Training these models can be done either from scratch using specific medical images or through transfer learning with pre-trained models (Huynh et al., 2016; Wang, 2024). Even if we can find several CNN-based systems that approached the breast cancer classification problems (e.g. (Dabass et al., 2023; Melekoodappattu et al., 2022; Razali et al., 2023)), they considered both MLO and CC views in the processing pipeline, without analyzing the contribution of each view to the prediction process.

<sup>1</sup>Breast Cancer Screening and Mammograms <https://www.bcrf.org/blog/mammogram-breast-cancer-screening-research/>

### 3 MATERIALS AND METHODS

#### 3.1 Dataset

In our pipeline, we utilized images from the Digital Database for Screening Mammography (CBIS-DDSM) (Sawyer-Lee et al., 2017), focusing specifically on cropped images to enhance the quality of the data.

Curated Breast Imaging Subset DDSM (CBIS-DDSM) is a dataset that contains mammograms from 6775 patients (Sawyer-Lee et al., 2017). It consists of images that contain abnormalities of type mass and calcification and the mammograms were taken from a CC view and also from a MLO view. The images are categorized into two primary classes: calcification and mass. Each of these classes is further subdivided based on the view, either craniocaudal (CC) or mediolateral oblique (MLO). Subsequently, these categories are further classified into benign, malignant, and benign without callback. A detailed description related to the number of images from each class can be seen in Table 1.

Table 1: Description of CBIS-DDSM dataset.

Abnormality	View	Tumor type	No of img
calcification	CC	benign	308
		malign	318
		b_w_c	262
	MLO	benign	350
		malign	355
		b_w_c	279
mass	CC	benign	367
		malign	363
		b_w_c	54
	MLO	benign	404
		malign	421
		b_w_c	87

For our approach, we decided to not include the mammograms that are from class benign without callback, as they do not require further immediate follow-up or additional diagnostic procedures, and the ones that contain both a benign and malign tumor, as they are not clear in which class to be included. After the exclusion of these cases, we have the number of images from each class as described in Table 2. For the experiments performed, we used the Region of Interest (ROI) from the images.

#### 3.2 Data Pre-Processing

The preprocessing phase involved applying two key techniques: Contrast Limited Adaptive Histogram

Table 2: Number of images from each class after triage.

Abnormality	View	Tumor type	No of img
calcification	CC	benign	362
		malign	281
	MLO	benign	176
		malign	164
mass	CC	benign	347
		malign	342
	MLO	benign	554
		malign	552

Equalization (CLAHE) and gamma correction.

CLAHE (Zuiderveld, 1994) is a method used to improve the contrast of images by limiting the amplification of noise. Gamma correction (Pedregosa et al., 2011) is a non-linear operation used to encode and decode luminance or tristimulus values in images. It adjusts the brightness of an image, enhancing the visibility of features by using a power-law transformation.

#### 3.3 Feature Extraction

Following preprocessing, we extracted a set of texture features that are crucial for characterizing the properties of the mammographic images. These included the Gray Level Co-occurrence Matrix (GLCM), Gray Level Run Length Matrix (GLRLM), and Gray Level Size Zone Matrix (GLSZM) (Tourassi, 1999). GLCM is a statistical method that examines the spatial relationship of pixels and is used to extract second-order texture information. GLRLM measures the occurrence of consecutive pixels with the same gray level value in specified directions, providing insights into the texture's fineness and coarseness. GLSZM analyzes the size of homogeneous zones in an image, indicating the distribution and prevalence of different zone sizes (van Griethuysen J. J. M., 2017).

#### 3.4 Machine Learning Model

After extracting the relevant features, we applied a residual network to the data. ResNet (Kaiming He and Sun, 2016) is a type of deep neural network that uses skip connections or shortcuts to jump over some layers. This architecture helps mitigate the vanishing gradient problem, allowing the network to learn deeper representations.

A bunch of previous experiments have indicated that the ResNet architecture is a promising one for the problem of breast cancer classification (Iacob and Diosan, 2024). The results obtained by ResNet were more robust than those obtained by other architectures (e.g. VGG, EfficientNet). Consequently, we focused

our investigations solely on ResNet for further analysis and refinement.

ResNET101 network with pretrained weights on the ImageNet dataset and Adam optimizer with various learning rates were involved in the experiment. We looked for the appropriate learning rate to use by trying heuristically different values in intervals  $1e-2$  and  $1e-6$ . After checking the results obtained, we decided to use  $1e-5$  as the learning rate for the experiments. Adam's adaptive learning rate mechanism adjusts the learning rates for each parameter individually based on the historical gradients, allowing for smoother and more stable training. Also, Adam optimizer provides consistent performance across different tasks and datasets, making it a reliable choice for a wide range of deep learning applications. For this reason, we consider using the Adam optimizer.

### 3.5 Training Procedure

The DDSM dataset was split into subsets based on view and the combinations used to create the subsets for the experiments can be seen in Figure 1. To validate our model, we employed a 5-fold cross-validation technique, which involves partitioning the dataset into five distinct folds, training the model on four folds, and validating it on the remaining fold. This process is repeated five times, each time with a different fold serving as the validation set.

Finally, we computed the average scores across each fold to evaluate the overall performance of our model, ensuring a robust and reliable assessment of the classifier's ability to detect and classify abnormalities in mammographic images. The scores used to measure the performance of the model are accuracy, sensitivity and specificity (Pedregosa et al., 2011).

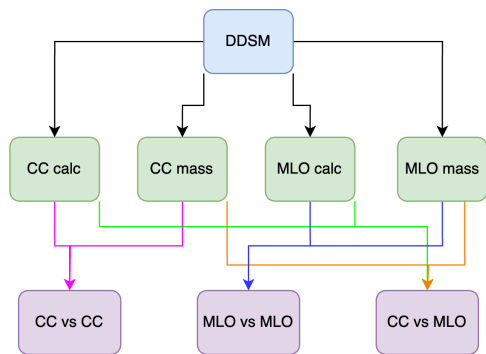


Figure 1: Combinations performed based on view for the experiments.

## 4 RESULTS AND DISCUSSIONS

Each of these two views, MLO and CC, has its advantages. The center and medial (inner) portions of the breast, particularly the region next to the chest wall, are visible in the CC view. The deep medial breast tissue, which is occasionally obscured by other views, is best visualized in this view. A greater area of the breast tissue is captured by MLO view, including the axillary (underarm) region and the upper outer quadrant, which are known to be breast cancer hotspots. Most breast tissue can be seen in the MLO view, even in places where the CC view might not be able to fully display it. In this context, the first analysis considers only the craniocaudal (CC) view and tries to differentiate cancer from benign based on mass-type abnormalities and calcification-type abnormalities, while the second analysis focuses on the MLO view with a similar aim. In all the experiments, different pre-processing steps have been performed on the raw images and various texture features have been extracted.

The purpose of the first experiment is to analyze the CC images to identify the best feature, determine which pre-processing method gives the best results, and check whether calcified lesions are easier to detect compared to those of the mass type. The second experiment focuses exclusively on the analysis of MLO images. In the third experiment, the performance between CC and MLO images is compared to understand the differences in lesion identification depending on the projection used.

The analysis of the results was carried out on three essential plans to ensure a complete and rigorous evaluation. The first plan focuses on identifying abnormalities in the data to detect any significant deviations from expected behaviour. The second plan aims to identify the most efficient method of data preprocessing, evaluating the impact of each type of preprocessing on model robustness. Finally, the third plan analyzes the best results obtained from the perspective of features, identifying the combinations of features that contribute the most to improving the performance of the model.

For each case of evaluation, we take into account an analysis based on accuracy, sensitivity and specificity. We will note the true positive cases with TP, true negative cases with TN, false positive cases with FP and false negative cases with FN.

$$accuracy = \frac{TN + TP}{TN + FP + TP + FN} \quad (1)$$

$$sensitivity = \frac{TP}{FN + TP} \quad (2)$$

$$specificity = \frac{TN}{TN + FP} \quad (3)$$

The accuracy formula is described in Equation 1 and alone is not sufficient, as it can be misleading in the case of unbalanced classes, where a model may appear to perform well only because it predicts the majority of the dominant class correctly. Sensitivity presented in Equation 2 is important to evaluate how well the model identifies positive cases, essential in detecting lesions, and specificity as in Equation 3 measures how well the model identifies negative cases, reducing false alarms. Using all three metrics accuracy, sensitivity and specificity we obtain a balanced evaluation of the model's performance, both in the correct detection of lesions and in avoiding errors.

Statistical analysis of the data for the three main texture features indicates that both the mean and standard deviation are within normal limits, suggesting a suitable distribution of values. The standard deviation, a key indicator of data variation, does not tend to zero, meaning that the data is not too concentrated around the mean, reflecting a healthy diversity of values<sup>2</sup>.

Table 3 and Table 4 will present the results obtained on the experiments. We marked with bold the maximum values for calcification and with italics the maximum values for mass.

#### 4.1 Experiment 1

Based on the experiments comparing the performance of calcification and mass detection in CC views, several observations were made regarding the metrics of accuracy, sensitivity, and specificity. The results of the experiments can be seen in Table 3.

The analysis revealed that calcifications consistently showed superior performance in accuracy across all seven evaluated features and for all preprocessing steps. This indicates a high level of reliability in correctly identifying the presence of calcifications compared to masses. For the detection of masses, the application of Contrast Limited Adaptive Histogram Equalization (CLAHE) led to improved results in only 2 out of 7 cases, suggesting that this preprocessing technique has limited effectiveness in enhancing the accuracy of mass detection.

The results for sensitivity, which measures the ability to identify true positive cases correctly, showed that calcifications outperformed mass in 4 out of 7 feature-based cases. This demonstrates a stronger

capability in identifying true positives for calcifications compared to masses. Notably, the combination of texture features, GLCM, GLRLM and GLSZM, provided the best sensitivity results for both calcifications and masses. However, the use of preprocessing techniques like CLAHE showed improvements in only 5 out of 14 cases, indicating that such methods do not consistently enhance sensitivity for either type of abnormality.

In terms of specificity, which measures the ability to identify true negatives correctly, calcifications again demonstrated better results in 6 out of 7 cases. This suggests a greater accuracy in distinguishing non-pathological cases. The application of CLAHE showed some benefits, improving specificity in 4 out of 14 cases, but its overall impact was limited.

#### 4.2 Experiment 2

Based on the comparison of the MLO view for calcification and mass detection, several key findings were observed regarding accuracy, sensitivity, and specificity. Results of the experiments are present in Table 4.

In the MLO view, calcifications consistently showed superior performance in accuracy, outperforming masses in all seven evaluated cases. This indicates a high reliability in correctly identifying calcifications over masses in this view. The combination of three specific texture features, GLCM, GLRLM and GLSZM, led to the best results, highlighting the importance of these features in accurate detection. Additionally, the application of CLAHE improved accuracy in mass detection in 3 out of 7 cases, suggesting some benefit in enhancing the clarity and contrast of mass images.

The sensitivity analysis revealed that calcifications had better results than masses in 6 out of 7 cases, indicating a more reliable identification of true positive cases for calcifications in the MLO view. For masses, the use of CLAHE improved sensitivity in 4 out of 7 cases, showing that this preprocessing technique can enhance the detection rate of true positives for masses in some instances.

The assessment of specificity showed that calcifications performed better than masses in 2 out of 7 cases. This indicates a more limited differentiation advantage for calcifications over masses in this metric.

#### 4.3 Experiment 3

The comparison between craniocaudal and MLO views for detecting calcifications in mammographic

<sup>2</sup>Results of the statistical analysis of data <https://github.com/biancalixandru0/Mean-and-standard-deviation>.

Table 3: Results (in terms of accuracy, sensitivity and specificity) for malign vs. benign (this is actually the classification problem) based on different tumor types (calc and mass) in CC images and by using various texture features. Sensitivity and specificity are computed as a micro-average over both classes.

		accuracy			sensitivity			specificity		
		none	gamma	clahe	none	gamma	clahe	none	gamma	clahe
CC calc	glcm	0.660	0.642	0.659	0.480	0.503	0.523	0.793	0.750	0.765
	glrlm	0.795	0.731	0.738	0.778	0.667	0.616	0.809	0.780	0.834
	glszm	0.692	0.658	0.652	0.479	0.447	0.433	0.858	0.822	0.822
	glcm_glrlm	0.751	0.701	0.688	0.680	0.578	0.501	0.806	0.796	0.832
	glcm_glszm	0.706	0.685	0.697	0.488	0.451	0.529	<b>0.875</b>	0.866	0.828
	glrlm_glszm	0.781	0.735	0.728	0.696	0.626	0.597	0.847	0.819	0.829
	glcm_glrlm_glszm	<b>0.817</b>	0.763	0.762	<b>0.780</b>	0.668	0.666	0.845	0.836	0.837
CC mass	glcm	0.590	0.597	0.611	0.378	0.481	0.473	0.798	0.711	0.747
	glrlm	0.721	0.678	0.674	0.738	0.653	0.613	0.700	0.702	0.734
	glszm	0.598	0.600	0.602	0.450	0.465	0.449	0.745	0.733	0.753
	glcm_glrlm	0.714	0.655	0.655	0.743	0.656	0.705	0.686	0.654	0.605
	glcm_glszm	0.626	0.612	0.620	0.517	0.518	0.588	0.734	0.705	0.652
	glrlm_glszm	0.705	0.664	0.645	0.699	0.643	0.614	0.712	0.684	0.675
	glcm_glrlm_glszm	0.733	0.693	0.666	0.740	0.696	0.629	0.725	0.689	0.702

Table 4: Results (in terms of accuracy, sensitivity and specificity) for malign vs. benign (this is the classification problem) based on different tumor types (calc and mass) in MLO images and by using various texture features. Sensitivity and specificity are computed as a micro-average over both classes.

		accuracy			sensitivity			specificity		
		none	gamma	clahe	none	gamma	clahe	none	gamma	clahe
MLO calc	glcm	0.675	0.621	0.600	0.472	0.365	0.506	<b>0.865</b>	0.860	0.726
	glrlm	0.806	0.773	0.740	<b>0.826</b>	0.751	0.763	0.787	0.793	0.719
	glszm	0.709	0.642	0.660	0.588	0.550	0.602	0.821	0.728	0.713
	glcm_glrlm	0.793	0.726	0.690	0.785	0.676	0.663	0.801	0.774	0.715
	glcm_glszm	0.735	0.686	0.713	0.631	0.587	0.622	0.832	0.778	0.798
	glrlm_glszm	0.828	0.758	0.708	0.804	0.669	0.619	0.851	0.842	0.791
	glcm_glrlm_glszm	<b>0.852</b>	0.759	0.757	0.847	0.715	0.682	0.857	0.801	0.827
MLO mass	glcm	0.588	0.552	0.566	0.744	0.765	0.779	0.429	0.333	0.347
	glrlm	0.744	0.654	0.723	0.736	0.597	0.717	0.752	0.712	0.729
	glszm	0.616	0.595	0.609	0.579	0.586	0.599	0.653	0.604	0.620
	glcm_glrlm	0.697	0.617	0.672	0.729	0.617	0.717	0.664	0.617	0.626
	glcm_glszm	0.615	0.597	0.616	0.577	0.636	0.588	0.655	0.557	0.645
	glrlm_glszm	0.694	0.669	0.721	0.676	0.650	0.741	0.712	0.688	0.700
	glcm_glrlm_glszm	0.707	0.686	0.733	0.703	0.711	0.760	0.711	0.660	0.705

imaging can be seen in Table 3 and Table 4 and reveals distinct differences in performance across various metrics.

When comparing the accuracy of CC and MLO views for calcifications, it was found that the best results were consistently obtained using a combination of GLCM, GLRLM and GLSZM features. This combination proved effective in both views. However, the MLO view provided better accuracy in all seven cases compared to the CC view, suggesting that the MLO view may offer superior visualization or positioning advantages for detecting calcifications.

The sensitivity analysis, also showed that the combination of GLCM, GLRLM, and GLSZM features

yielded the best results for both CC and MLO views. Nonetheless, the MLO view demonstrated superior sensitivity in 6 out of 7 cases compared to the CC view. This indicates that the MLO view may be more reliable for detecting the presence of calcifications.

In terms of specificity, the MLO view again outperformed the CC view in 4 out of 7 cases. While the difference in specificity between the views was less pronounced than in accuracy and sensitivity, the MLO view still showed an advantage in distinguishing non-pathological cases.

Following the analysis of the craniocaudal versus MLO views for calcifications, we turn to the comparison of these views for detecting masses in mammo-

graphic imaging. The results, as summarized in Tables 3 and Table 4, provide insights into the performance of these views.

In evaluating the accuracy of CC versus MLO views for detecting masses, it was found that the combination of GLCM, GLRLM and GLSZM features yielded the best results for the CC view. The CC view outperformed the MLO view in 5 out of 7 cases, indicating a generally higher accuracy in mass detection when using the CC view.

The sensitivity analysis revealed that the CC view provided better results than the MLO view in 4 out of 7 cases. Notably, the use of CLAHE as a preprocessing technique in the MLO view improved sensitivity outcomes in 5 out of 7 cases, demonstrating the potential benefit of this method in enhancing the visibility and detection of masses. Overall, the application of preprocessing methods was advantageous in 8 out of 14 cases, suggesting a moderate but noteworthy improvement in detection capability.

When assessing specificity, the CC view again showed superior results, outperforming the MLO view in 6 out of 7 cases. This suggests that the CC view may be more effective in avoiding false positives when evaluating masses.

We conducted experiments to determine whether the type of abnormality—calcification or mass—impacts detection performance. Unfortunately, we were unable to achieve an accuracy above 70% in any of the cases tested. Consequently, we excluded these results from this section. However, our findings underscore the importance of considering the type of abnormality to enhance performance.

## 5 CONCLUSIONS

The findings suggest that calcifications are generally more reliably detected and characterized than masses in CC mammographic views. The consistent use of the GLCM, GLRLM, and GLSZM feature combination plays a crucial role in enhancing diagnostic accuracy and sensitivity. However, the application of preprocessing techniques like CLAHE shows only case-dependent benefits, particularly for mass detection. Overall, these insights underscore the importance of targeted feature selection and highlight the more robust diagnostic performance for calcifications.

Calcifications are generally detected with higher accuracy and sensitivity in the MLO view compared to masses. The use of specific texture features, particularly those including GLRLM, is crucial for achieving the best diagnostic outcomes. While the application of CLAHE shows some benefits, particularly in

improving sensitivity for mass detection, its overall impact varies. These results highlight the importance of feature selection and preprocessing techniques in enhancing the detection and characterization of breast abnormalities in mammographic imaging.

Furthermore, images exhibiting calcification abnormalities demonstrate better performance overall compared to those containing mass abnormalities.

## REFERENCES

- Abdolell, M., Payne, J. I., Caines, J., Tsuruda, K., Barnes, P. J., Talbot, P. J., Tong, O., Brown, P., Rivers-Bowerman, M., and Iles, S. (2020). Assessing breast cancer risk within the general screening population: developing a breast cancer risk model to identify higher risk women at mammographic screening. *European Radiology*, 30:5417–5426.
- Araque, O., Mejía-Sandoval, M., Sassi, A., Holli-Helenius, K., Lääperi, A.-L., Rinta-Kiikka, I., Arponen, O., and Pertuz, S. (2019). Selecting the mammographic-view for the parenchymal analysis-based breast cancer risk assessment.
- Astrid Padilla, Otso Arponen, I. R.-K. S. P. (2021). Image retrieval-based parenchymal analysis for breast cancer risk assessment. *The International Journal of Medical Physics Research and Practice*, 49.
- Bajcsi, A. and Chira, C. (2023). Textural and shape features for lesion classification in mammogram analysis. In *International Conference on Hybrid Artificial Intelligence Systems*, pages 755–767.
- Bassett, L. W. (1992). Mammographic analysis of calcifications. *Radiologic Clinics of North America*, 30(1):93–105.
- Charan, S., Khan, M. J., and Khurshid, K. (2018). Breast cancer detection in mammograms using convolutional neural network. In *2018 International Conference on Computing, Mathematics and Engineering Technologies (iCoMET)*, pages 1–5.
- Coughlin, S. S. and Ekwueme, D. U. (2009). Breast cancer as a global health concern. *Cancer Epidemiology*, 33(5):315–318.
- Cui, Y., Li, Y., Xing, D., Bai, T., Dong, J., and Zhu, J. (2021). Improving the prediction of benign or malignant breast masses using a combination of image biomarkers and clinical parameters. *Frontiers in Oncology*, 11:629321. Erratum in: *Front Oncol*. 2021 Apr 29;11:694094. doi: 10.3389/fonc.2021.694094.
- Dabass, J., Dabass, M., and Dabass, B. S. (2023). Fuzzydeepnets based feature extraction for classification of mammograms. *Intelligence-Based Medicine*, 8:100117.
- Duffy, S., Nagtegaal, I., Astley, S., Gillan, M., McGee, M., Boggis, C., Wilson, M., Beetles, U., Griffiths, M., Jain, A., Johnson, J., Roberts, R., Deans, H., Duncan, K., Iyengar, G., Griffiths, P., Warwick, J., Cuzick, J., and Gilbert, F. (2008). Visually assessed breast den-

- sity, breast cancer risk and the importance of the cranio-caudal view. *Breast cancer research : BCR*, 10:R64.
- Huynh, B. Q., Li, H., and Giger, M. L. (2016). Digital mammographic tumor classification using transfer learning from deep convolutional neural networks. *Journal of Medical Imaging*, 3(3):034501.
- Iacob, B. and Diosan, L. (2024). Exploring the fusion of cnns and textural features in mammogram interpretation. *International Conference on Knowledge-Based and Intelligent Information & Engineering Systems*.
- Kaiming He, Xiangyu Zhang, S. R. and Sun, J. (2016). Deep residual learning for image recognition. *2016 IEEE Conference on Computer Vision and Pattern Recognition (CVPR)*, pages 770–778.
- Kala, S. and Ezhilarasi, M. (2018). Fusion of k-gabor features from medio-lateral-oblique and cranio-caudal view mammograms for improved breast cancer diagnosis. *Journal of Cancer Research and Therapeutics*, 14.
- Kim SJ, Moon WK, C. N.-C. J. K. S. I. J. (2006). Computer-aided detection in digital mammography: comparison of cranio-caudal, mediolateral oblique, and mediolateral views. *Radiology*.
- Mahmood, T., Li, J., Pei, Y., Akhtar, F., Rehman, M. U., and Wasti, S. H. (2022). Breast lesions classifications of mammographic images using a deep convolutional neural network-based approach. *PLOS ONE*, 17(1):e0263126.
- Melekoodappattu, J. G., Dhas, A. S., Kandathil, B. K., and Adarsh, K. S. (2022). Breast cancer detection in mammogram: combining modified cnn and texture feature based approach. *Journal of Ambient Intelligence and Humanized Computing*, 14(1):11397–11406.
- Pedregosa, F., Varoquaux, G., Gramfort, A., Michel, V., Thirion, B., Grisel, O., Blondel, M., Prettenhofer, P., Weiss, R., Dubourg, V., Vanderplas, J., Passos, A., Cournapeau, D., Brucher, M., Perrot, M., and Duchesnay, E. (2011). Scikit-learn: Machine learning in Python. *Journal of Machine Learning Research*, 12:2825–2830.
- Pérez-Benito, F. J., Signol, F., Pérez-Cortés, J.-C., Pollán, M., Pérez-Gómez, B., Salas-Trejo, D., Casals, M., Martínez, I., and Llobet, R. (2019). Global parenchymal texture features based on histograms of oriented gradients improve cancer development risk estimation from healthy breasts. *Computer Methods and Programs in Biomedicine*, 177:123–132.
- Razali, N. F., Isa, I. S., Sulaiman, S. N., Karim, N. K. A., and Osman, M. K. (2023). Cnn-wavelet scattering textural feature fusion for classifying breast tissue in mammograms. *Biomedical Signal Processing and Control*, 83:104683.
- Rodriguez-Ruiz, A., Lång, K., Gubern-Merida, A., Broeders, M., Gennaro, G., Clauser, P., Helbich, T. H., Chevalier, M., Tan, T., Mertelmeier, T., et al. (2019). Stand-alone artificial intelligence for breast cancer detection in mammography: comparison with 101 radiologists. *JNCI: Journal of the National Cancer Institute*, 111(9):916–922.
- Sasikala, S. and Arun Kumar, S. (2024). Enhancement of breast cancer screening through texture and deep feature fusion model using mlo and cc view mammograms. In *Exploration of Artificial Intelligence and Blockchain Technology in Smart and Secure Healthcare Advances in Computing Communications and Informatics*, volume 7, page 96.
- Sawyer-Lee, R., Gimenez, F., Hoogi, A., and Rubin, D. (2017). Curated breast imaging subset of digital database for screening mammography (cbis-ddsm). *International Research and Innovation Summit (IRIS2017)*.
- Singh, H., Sharma, V., and Singh, D. (2022). Comparative analysis of proficiencies of various textures and geometric features in breast mass classification using k-nearest neighbor. *Visual Computing for Industry, Biomedicine, and Art*, 5(1):3.
- Siviengphanom, S., Gandomkar, Z., Lewis, S. J., and Brennan, P. C. (2022). Mammography-based radiomics in breast cancer: a scoping review of current knowledge and future needs. *Academic Radiology*, 29(8):1228–1247.
- Tan, M., Zheng, B., Leader, J. K., and Gur, D. (2016). Association between changes in mammographic image features and risk for near-term breast cancer development. *IEEE Transactions on Medical Imaging*, 35(7):1719–1728. Epub 2016 Feb 11.
- Tourassi, G. D. (1999). Journey toward computer-aided diagnosis: role of image texture analysis. *Radiology*, 213(2):317–320.
- Vachon, C. M., Brandt, K. R., Ghosh, K., Scott, C. G., Maloney, S. D., Carston, M. J., Pankratz, V. S., and Sellers, T. A. (2007). Mammographic breast density as a general marker of breast cancer risk. *Cancer Epidemiology Biomarkers & Prevention*, 16(1):43–49.
- van Griethuysen J. J. M., Fedorov A., P. C. H. A. A. N. N. V. B.-T. R. G. H. F.-R. J. C. P. S. A. H. J. W. L. (2017). Computational radiomics system to decode the radiographic phenotype. *Cancer Research*, pages e104–e107.
- Van Timmeren, J. E., Cester, D., Tanadini-Lang, S., Alkadhi, H., and Baessler, B. (2020). Radiomics in medical imaging—“how-to” guide and critical reflection. *Insights into imaging*, 11(1):91.
- Wang, L. (2024). Mammography with deep learning for breast cancer detection. *Frontiers in Oncology*, 14.
- Zuiderveld, K. (1994). Contrast limited adaptive histogram equalization. *Graphics gems*, 4:474–485.